Optical and Quantum Electronics **11** *(1979) 153–160*

An unstable resonator Nd–YAG laser

D. C. HANNA, L. C. LAYCOCK
Department of Electronics, University of Southampton, Highfield, Southampton, UK

Received 18 August 1978

The operating characteristics of an unstable resonator Q-switched Nd–YAG laser are reported and its suitability for a number of applications has been tested. At repetition rates up to 50 Hz, output energies of 150–200 mJ are obtained with a beam divergence of 0.25 mrad half-angle. Single longitudinal mode operation has been achieved either with passive Q-switching or with an active slow Q-switch.

1. Introduction

Unstable resonator configurations have been extensively used on CO_2 lasers for many years. More recently Ewanizky and Craig [1] and Herbst *et al.* [2] have shown that the technique can also be successfully applied to a Q-switched Nd–YAG laser, and obtained a much greater output than could be achieved with a stable resonator. However the output beam in the near-field is then in the form of an annulus and for a number of applications this would at first sight appear less suitable than a Gaussian beam. In this paper we describe the results of a detailed investigation of the output characteristics of a Q-switched Nd–YAG laser and an examination of the suitability of the output beam for a number of applications. These include pumping a parametric oscillator, generation of second harmonic radiation (and its subsequent use to pump a dye laser), and generation of a coherent anti-Stokes Raman signal (CARS). In each case it was found that the generated signal was much greater than could be obtained when the same laser operated with a stable resonator. In some applications (e.g. holography) it is important to have single longitudinal mode operation of the Nd–YAG laser. In a stable resonator this is customarily achieved with the help of etalons or resonant reflectors. The application of such techniques to an unstable resonator is less straightforward since the beam within the resonator is not collimated. We have shown that by using a previously reported slow Q-switching technique [3, 4], it is possible to obtain single longitudinal mode operation from an unstable resonator with a single frequency-selecting etalon. We have also obtained similar results with a saturable absorber Q-switch.

2. Resonator design

The laser used in these experiments was a JK System 2000. The 3 inch × $\frac{1}{4}$ inch Nd–YAG rod was pumped by a single linear flashlamp in a diffusely reflecting ceramic pump chamber arrangement, which appears to give satisfactory pumping uniformity. With a stable resonator, the Q-switched output was typically 15 mJ in the TEM_{00} mode.

Siegman [5] has outlined the design approach for an unstable resonator and we have followed his suggested procedure. The basic design chosen was a positive branch confocal resonator since the positive branch avoids having a beam focus within the resonator and the confocal arrangement offers the convenience of a collimated output. In practice the performance of the laser was found to be fairly insensitive to departure from the calculated design parameters. In particular, no significant change in output beam quality was observed when the equivalent Fresnel number was varied from half integer to whole integer values. It is important however to include in the design the effects of thermal lensing of the laser rod, as pointed out by Herbst *et al.*, since this considerably modifies the parameters of the empty resonator. With the limited range of mirrors available the best performance was obtained with the resonator shown in Fig. 1, the Q-switched output being typically ~ 170 mJ. This resonator was confocal (i.e. gave a collimated output) for a 75 cm mirror spacing at a 30 Hz pump repetition rate. The rod focal length was ~ 3.5 m under these conditions. At 40 Hz, the

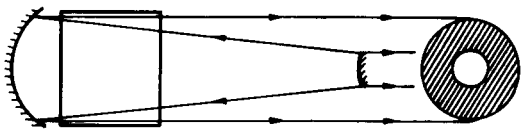

Figure 1 Unstable resonator configuration, for confocal operation (i.e. collimated output) at 30 Hz pump repetition rate. Convex mirror, 60 cm radius of curvature, diameter 1.8 mm; concave mirror, 5 m radius of curvature; laser rod centre 30 cm from concave mirror; mirror spacing, 75 cm.

increased thermal lensing required a cavity length reduction of ~ 15 cm to maintain the confocal condition. With a stable resonator the beam parameters are less influenced by thermal lensing of the laser rod. However, it should be pointed out that to obtain the same 170 mJ output from a stable resonator it would be necessary to use an oscillator/amplifier combination and the amplified beam parameters would then show a dependence on repetition rate similar to that of the unstable resonator.

Three different arrangements have been used for the small mirror (see Fig. 2). In the first (Fig. 2a) the output coupling was achieved by a highly reflecting (dielectric coated) inclined surface with a hole of ~ 1.8 mm diameter through it to allow access to the convex resonator mirror. Rather than use a plate with a hole drilled through it (which gives rather ragged edges to the hole) we have used a piece of quartz capillary tubing, cut at ~ 45° and then polished and coated. A very clean edge to the hole is obtained in this way. In the second arrangement the piece of capillary tubing was optically contacted to a prism. Total internal reflection occurs where the capillary hole meets the prism and the annular output is then extracted through the capillary, in line with the resonator axis. Both of these arrangements gave

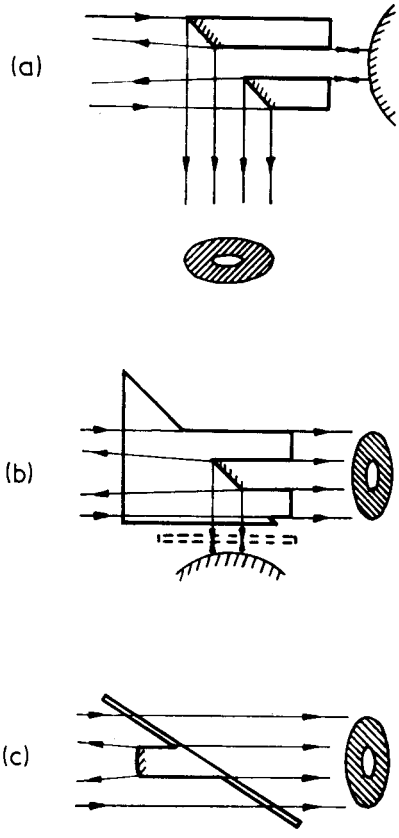

Figure 2 Three designs of output coupler arrangement, shown in cross-section. When a saturable absorber Q-switch was used, best operation occurred with the absorber placed in the position indicated by the dotted lines.

good results and have the advantage that a standard size of convex mirror substrate can be used. A further advantage of these arrangements was found when the saturable absorber Q-switch was used. When the absorber was placed just in front of the convex mirror (see Fig. 2b) it was exposed to a more uniform illumination and gave a better beam quality than when placed in the full beam. The best output energies were however achieved with the small diameter dielectric-coated convex mirror, which was cemented to a Brewster's angle supporting window. This arrangement was used by Herbst *et al.* The results discussed below were obtained with this mirror.

3. Beam quality

Beam profile measurements have been made either with a scanning slit or using a linear photodiode array, consisting of 100 silicon photodiodes occupying a total length of 1 cm. A typical near-field profile, taken with the diode array at about 50 cm from the small mirror, is shown in Fig. 3. There are two features worth noting. Firstly, it can be seen that the intensity is not radially uniform over the annulus (which the simpler analyses usually assume it to be). Secondly, it can be seen that an intense spot has developed in the centre of the beam. This is the so-called Poisson spot (see, for example, Klein [6]) and will be discussed later. In the far-field, the pattern changes to a central spot (an Airy disc) surrounded by much weaker rings. The beam profile then showed little change beyond a distance of 9 m, so measurements of far-field characteristics were made at this distance. The energy content of the far-field central spot was measured to be 60% of the total output and the half-angle subtended by the first dark ring was found to be 0.25 mrad. By comparison the calculated values assuming a uniform field over an annulus of 1.8 mm internal and 6.3 mm external diameter are 70% and 0.17 mrad, respectively.

For some applications the annular beam profile of the near-field is acceptable. For example, we have found that the near-field beam can be used for efficient second harmonic generation (see Section 4.2). There are other situations however where the far-field beam profile is more suitable, such as where the beam is to pass through an amplifier, or where it is used to pump a parametric oscillator (see Section 4.1). If the beam is allowed to propagate freely, the far-field distance can be roughly defined as the distance at which the collimated beam leaving the resonator is seen to occupy one Fresnel zone. For a uniform near-field intensity over an annulus with internal and external radii, a_1, and Ma_1, respectively, this distance is $a_1^2(M^2 - 1)/\lambda$. For our experimental conditions this works out to be ~ 9 m. To reduce this to a more convenient distance we have tried using a beam reducing telescope (3×), the far-field distance being thus reduced by 3^2, and then following this with an identical telescope to expand the beam to its former size. However, problems were encountered with damage to the AR coatings of the exit lens of the first telescope. In fact we have so far found the most satisfactory arrangement to be a simple folding of the beam by multiple reflections between a pair of parallel plane mirrors.

As the beam propagates to the far-field a bright Poisson spot develops at the centre of the beam. As shown in textbooks on optics (e.g. Klein [6]) the intensity of the spot can reach a value four

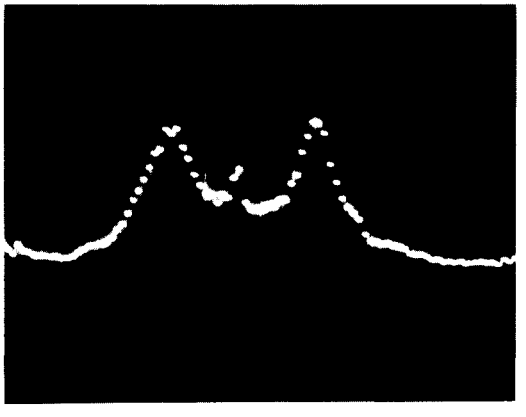

Figure 3 Intensity profile, monitored by photodiode array in the near-field. The small central maximum is the Poisson spot.

times that of the near-field intensity for the case where the near-field intensity is uniform over the annulus. Since this could lead to serious damage problems when components are placed in the beam, we have made measurements of the Poisson spot intensity. In fact it was found that the maximum intensity reached by the spot was no greater than the maximum near-field intensity. The explanation for the low intensity of the spot lies in the radially non-uniform intensity of the near-field. Treacy [7] has analysed the behaviour of the Poisson spot for a near-field profile with a Gaussian radial dependence (spot size w) but with zero field over a central disc of diameter $2a_1$. This represents a rough approximation to the actual profile we observed except that the Gaussian does not include the feature of truncation at the outer diameter of the beam. Treacy showed that the on-axis intensity at a distance L is given by

$$I(0,L) \propto |E(0,L)|^2 = A^2 e^{-2a_1^2/w^2} [1 + (1/\pi^2 N^2)]^{-1} \quad (1)$$

where

$$N = w^2/\lambda L \quad (2)$$

the near-field distribution being given by

$$I(r,0) \propto |E(r,0)|^2 = \begin{cases} A^2 e^{-2r^2/w^2} & \text{for } r \geqslant a_1 \\ 0 & \text{for } r < a_1 \end{cases} \quad (3)$$

Obviously Equation 1 does not give a correct answer for very small L [since $E(0,L)$ should become zero as $L \to 0$, as Equation 3]. The explanation for this discrepancy is that the inclination factor (see Klein [6]) was not included in the calculation, although the result (Equation 1) should be valid for distances greater than several beam diameters. Also Equation 1 does not display any oscillation of Poisson spot intensity with distance along the beam axis since the Gaussian was not truncated at the outside diameter of the beam. However Equation 1 does show that as L decreases the maximum on-axis intensity does not exceed $A^2 \exp(-2a_1^2/w^2)$, which is the maximum intensity of the exit beam (on the inside rim of the annulus). This result shows that the low intensity of the Poisson spot is connected with the radial decrease of intensity in the near-field and it appears that a uniform near-field profile may be an actual disadvantage.

4. Some applications of the unstable resonator output

4.1. Pumping an optical parametric oscillator (OPO)

A comparison was made between the performance of a $LiNbO_3$ OPO, pumped at 1.06 μm by the unstable resonator output with that achieved using a TEM_{00} pump. About 80 mJ of TEM_{00} energy was available from a Q-switched stable resonator/amplifier combination. The performance of the OPO with this pump arrangement has been described elsewhere (Wyatt *et al.* [8]). When the OPO was pumped by ~ 80 mJ energy in the near-field of the unstable resonator beam the OPO performance was significantly worse, in contrast to the results reported by Herbst *et al.* [2]. This poor performance can be ascribed to the large double-refraction 'walk-off' by the extraordinary-polarized pump beam, about 2 mm over the 50 mm length of crystal. The hole in the pump distribution therefore tracks right across the central portion of the pump beam and parametric oscillation took place in two separate regions, one above and one below the central hole (see Fig. 4).

By allowing the pump beam to propagate ~ 9 m, it was found that the central Airy disc contained ~ 80 mJ of energy and had a diameter close to that of the amplified TEM_{00} beam. The subsidiary rings of this far-field distribution were removed by an aperture and it was found that the performance of the OPO pumped by this 80 mJ was the same as with the TEM_{00} pump. Thus the same results were achieved with an unstable Nd–YAG oscillator alone as with a stable oscillator/amplifier.

4.2. Second Harmonic generation

A KD^*P crystal, cut for type II phase-matching, was used for second harmonic generation. The double refraction 'walk-off' was much less than for the $LiNbO_3$ OPO and it was found that efficient SHG could be produced in the near-field, a typical energy conversion efficiency being ~ 25% for an input energy of 170 mJ. This represents about an order of magnitude increase in SH energy over that available using a stable oscillator. In fact the conversion efficiency was about half this value when the far-field beam was used. Again the question arises of whether the near-field SH distribution,

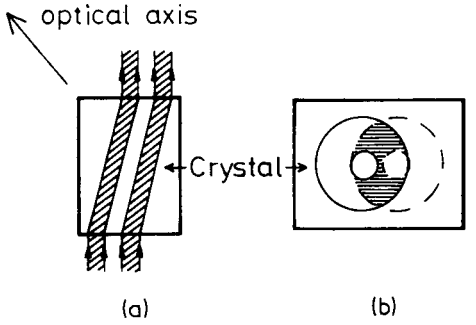

Figure 4 (a) Plan view showing double refraction walk-off by pump beam. (b) End view showing position of annular beam at input (solid circles) and output (dotted circles) of the crystal. Oscillation took place in the two hatched regions.

which has the same annular form as the fundamental beam, is as useful for subsequent applications as the far-field SH beam. We have therefore examined the efficiency of a Rhodamine 6G dye laser when pumped transversely by the near-field-generated SH beam. Two cylindrical lenses, with their axes orthogonal, were used to shape the pumped region in the dye cell of the oscillator. The first lens spread the beam in one plane to fill the ~ 1 cm width of the dye cell side window and the other lens focused the beam to form an elongated streak. Close examination of the beam shape at the cell revealed that it had the form of a 'squashed' annulus with a reduced, but not zero, intensity at the centre. Despite this pump distribution the dye oscillator performed well. With ~ 7 mJ of SH energy into the oscillator dye cell and ~ 18 mJ into an amplifier cell the dye laser output was 4 mJ. The beam was diffraction-limited (0.3 mrad half-angle divergence), with an approximately Gaussian intensity profile. Line-narrowing was achieved by means of a set of four prism beam expanders [9, 10] to present an elongated beam to the 3200 lines/mm holographic grating. The laser linewidth was measured to be 0.15 cm^{-1} and by adding an intracavity etalon this was reduced to 0.02 cm^{-1} (the laser energy falling to 3 mJ).

4.3. Coherent anti-Stokes Raman scattering (CARS)

The second harmonic of a Nd–YAG laser is widely used as one of the input beams in CARS experiments. One such set-up has been described by Beattie *et al.* [11] in which the second harmonic beam was produced by a Q-switched stable resonator Nd–YAG laser (also a JK system 2000), the other beam (at the lower frequency) coming from a flash-lamp pumped dye laser (CMX-4). The CARS signal should therefore be proportional to the square of the second harmonic beam intensity. To make a quantitative test of the effect of converting this Nd–YAG laser to an unstable resonator, the CARS signal from the vibrational Q branch of atmospheric nitrogen was observed. The second harmonic was generated in the near-field and then combined with the CMX-4 beam at a common focus. The CARS signal was found to be two orders of magnitude greater than the best obtained with the stable resonator. This is consistent with the order of magnitude increase in available SH power and confirms that the increased output from the unstable resonator can all be used effectively.

5. Single longitudinal mode selection

The usual technique for producing single longitudinal mode operation of a laser involves the use of one or more Fabry–Perot etalons. The etalon transmission depends on the angle of incidence and thus imposes more stringent requirements on the choice of etalon in an unstable resonator since the angular spread of the beam (for one direction of travel within the resonator) is much greater than for a typical TEM_{00} mode in a stable resonator. For example in the resonator we have described, the divergence half-angle $\theta_{1/2}$ of the beam reflected back from the small mirror is ~ 3 mrad whereas for a stable resonator Nd–YAG laser it would be typically 0.4 mrad.

To avoid large insertion losses and distortion of the intensity profile as the beam passes through the etalon it is necessary to ensure essentially the same transmission for all angular components of the beam and this implies the use of an etalon with a lower angular selectivity (e.g. a thinner etalon) in the case of an unstable resonator. This in turn implies a lower selectivity with respect to fre-

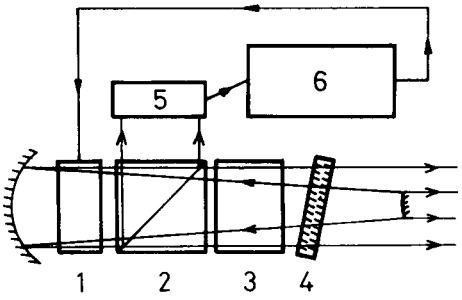

Figure 5 Laser resonator arrangement with slow Q-switch for single longitudinal mode operation. (1) Pockels cell, (2) Glan polarizer, (3) Nd–YAG rod, (4) etalon [(FSR) 3.3 cm^{-1}, F (finesse) = 7.5], (5) silicon photodiode, (6) triggering electronics.

quency. To obtain sufficient selectivity for single longitudinal mode operation we have therefore used a slow Q-switching technique which provides a very large number of passes through the etalon. This slow Q-switch scheme has been described in detail elsewhere, having originally been used for a stable resonator [3, 4], see Fig. 5. Briefly the principle can be summarized as follows. The Pockels cell Q-switch is used in a manner analogous to a saturable absorber, by initially keeping the cell partly open for the first 1000 or so passes through the resonator and then opening it completely when the laser intensity reached some predetermined value. During the large number of passes a single longitudinal mode is selected and this is subsequently amplified to the full output power after the Q-switch has been completely opened. The choice of etalon parameters (thickness t, refractive index μ and reflectivity R of its faces) is constrained by two requirements. First there must be enough selectivity so that in q round trips through the resonator, a single longitudinal mode is selected. As in [4] we at first adopt as our criterion of single mode selection the condition that the intensity of the selected mode should be at least ten times greater than that of adjacent modes. It is shown in [4], that this condition leads to the requirement

$$q\frac{8\pi^2\mu^2t^2R}{L^2(1-R)^2} > \log_e 10 \qquad (4)$$

where L is the length of the laser resonator. This can be expressed in the rather simpler form,

$$\frac{F}{(\mathrm{FSR})} \geqslant 1.07\, L/\sqrt{q} \approx L/\sqrt{q} \qquad (5)$$

where F is the finesse, and (FSR) is the free spectral range in wavenumbers. The second constraint is that transmission of the etalon should only show a small variation for the range of ray angles within the beam. Obviously the etalon should be aligned as close to normal incidence as possible, being offset by just enough (θ_{tilt}) to prevent oscillation, with the etalon acting as a resonator mirror.

We assume that for some angle θ within the range of angles of incidence presented by the beam there is exact Fabry–Perot resonance, thus,

$$2\mu t\cos(\theta/\mu) = m\lambda \qquad (6)$$

whereas at the two extremes, θ_1 and θ_2, of angles of incidence, the resonance is not exact, thus

$$\begin{aligned} 2\mu t(\cos\theta_1/\mu) &= (m+\epsilon)\lambda \\ 2\mu t(\cos\theta_2/\mu) &= (m-\epsilon)\lambda \end{aligned} \qquad (7)$$

where $\epsilon \ll 1$. Using the fact that the angles are small, Equations 7 can be combined to give

$$\epsilon = \frac{t}{2\lambda\mu}(\theta_2^2-\theta_1^2) = \frac{2t}{\lambda\mu}\theta_{1/2}\theta_{\mathrm{tilt}}. \qquad (8)$$

The transmission of the etalon for the angles of incidence θ_1, θ_2 is

$$T = \frac{1}{[1+(4F^2/\pi^2)\sin^2(\pi\epsilon)]} \approx 1-4F^2\epsilon^2 \qquad (9)$$

and taking the criterion that T should not be less than 0.9 for θ_1 and θ_2, the following condition is obtained

$$4F^2\epsilon^2 \leqslant \tfrac{1}{10} \qquad (10)$$

which, with the help of Equation 8 can be re-expressed as

$$\frac{F}{(\mathrm{FSR})} \leqslant \frac{\lambda\mu^2}{2\sqrt{10}\theta_{1/2}\theta_{\mathrm{tilt}}}. \qquad (11)$$

Thus Equations 5 and 11 together define the permitted limits for $F/(\mathrm{FSR})$ as

$$L/\sqrt{q} \lesssim \frac{F}{(\mathrm{FSR})} \leqslant \frac{\lambda\mu^2}{2\sqrt{10}\theta_{1/2}\theta_{\mathrm{tilt}}}. \qquad (12)$$

It was found experimentally that θ_{tilt} had to be set at ~ 6 mrad to avoid oscillation off the etalon. Thus with $\theta_{\mathrm{tilt}} = 6$ mrad, $\theta_{1/2} = 3$ mrad and $\mu \simeq 1.5$, the right-hand inequality becomes $F/(\mathrm{FSR}) \lesssim 2$ cm. On the other hand, with $q = 1000$, $L = 75$ cm, the left-hand inequality gives $F/(\mathrm{FSR}) \geqslant 2.4$ cm. Other considerations that go into the etalon design are the need to have a large enough (FSR) to avoid oscillation on two etalon maxima and the need to avoid very high values of finesse since the coatings are then liable to damage.

From the above numbers it can be seen that the prescribed criteria of mode-selectivity and insertion loss cannot quite be met for our laser, although with an etalon having $F/(\mathrm{FSR}) \approx 2$ cm the conditions are very nearly met. We have therefore chosen to use a fused silica etalon, of 1 mm thickness, with 65% reflectivity on both faces, thus giving $F/(\mathrm{FSR}) = 7.2/3.3 = 2.2$ cm. The etalon was placed in an oven on an angular mount. The face normal was tilted from the resonator axis until parasitic oscillation was suppressed. Care had also to be taken to tilt other components in the resonator (polarizer and Pockels cell) to avoid spurious frequency selection effects from their surfaces. The etalon temperature was then adjusted to minimize the threshold. This ensures that a maximum etalon transmission is coincident with the maximum of the laser gain profile. The insertion of the etalon reduced the output by around 20% typically. The longitudinal mode behaviour was monitored both by Fabry–Perot interferometer (after converting the 1.06 μm to its second harmonic for convenience) and by observing the degree of modulation at the $c/2L$ frequency when the output was detected by fast photodiode. With the etalon inserted and normal Q-switching used, a linewidth of around 0.1 cm^{-1}, was measured. By adjusting the Pockels cell voltage for slow Q-switching, reliable single longitudinal mode operation was indeed achieved, thus implying a linewidth of less than 0.01 cm^{-1}. This is consistent with an increase in q of more than two orders of magnitude since this, according to Equation 4, reduces the linewidth by more than an order of magnitude. This single mode output energy was typically 120 mJ.

Fig. 6 shows the Fabry–Perot rings monitored by means of the photodiode array. The two large peaks are separated by the 0.03 cm^{-1} (FSR) of the Fabry–Perot interferometer. The small subsidiary peaks are believed to be due to spurious additional reflections from the Fabry–Perot interferometer mirrors rather than due to adjacent longitudinal modes of the laser. In any case the photograph confirms that adjacent longitudinal modes have an intensity less than $\sim$ 15% of the selected mode and this is further confirmed by the fact that the observed intensity modulation at $c/2L$ observed on the fast photodiode was less than 10% of the overall intensity. A similar narrow linewidth was obtained using a saturable absorber Q-switch contained in a thin plastic film. The output energy was reduced however, both because the transmission of the quiescent absorber was too high and the transmission of the bleached absorber was not complete. As noted earlier, the performance was most reliable and the output beam quality was best when the absorber was placed as shown in

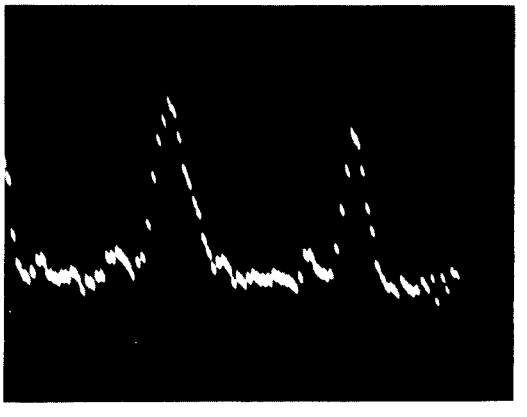

Figure 6 Fabry–Perot rings observed using photodiode array. Free spectral range, i.e. spacing between large peaks in display, is 0.03 cm^{-1}. Axial mode spacing of Nd–YAG laser, 0.006 cm^{-1} (calculated).

Fig. 2b. The reliable operation in this position suggests that with an appropriate saturable absorber it may be possible to obtain mode-locked operation of an unstable resonator Nd–YAG laser.

6. Conclusions

We have tested an unstable resonator Nd–YAG Q-switched laser in a number of typical applications. For ease of operation, and reliability, we have found this configuration to be just as good as a stable resonator. In some situations, e.g. pumping a parametric oscillator, it may be that only around 50% of the output of the unstable resonator can be used effectively. However the order of magnitude increase of diffraction-limited output compared to a stable resonator means that much more energy is available even in this least favourable of cases. We have also shown that single longitudinal mode operation can be achieved when slow Q-switching is used. The extra output energy is therefore available for applications such as holography, which require narrow linewidth operation.

Acknowledgements

We wish to acknowledge the help given by several people in the various experiments in which applications of the unstable resonator output were tested. These include Dr G. Kerr in the dye laser tests, Drs T. R. Gilson and D. Greenhalgh in the CARS experiment, and Mr A. J. Turner in the OPO tests, who also gave help with the slow Q-switch. We are particularly indebted to Dr J.K. Wright of JK Lasers who loaned the system 2000 laser and a number of extra optical components for this work. The loan of a plastic Q-switch by Dr D. H. Arnold of EMI is also gratefully acknowledged. This work has been supported partly by the Science Research Council and one of us (LL) holds an SRC studentship.

References

1. T. F. EWANIZKY and J. M. CRAIG, *Appl. Opt.* **15** (1976) 1465–69.
2. R. L. HERBST, H. KOMINE and R. L. BYER, *Opt. Commun.* **21**, (1977) 5–7.
3. D. C. HANNA, B. LUTHER-DAVIES and R. C. SMITH, *Electr. Lett.* 8 (1972) 369–70.
4. *Idem, Opto-Electronics* 4 (1972) 249–56.
5. A. E. SIEGMAN, *Laser Focus* (1971) 42–47.
6. M. V. KLEIN, 'Optics' (John Wiley and Sons Inc. 1970) p. 382.
7. E. B. TREACY, *Appl. Opt.* 8 (1969) 1107–9.
8. R. WYATT, A. J. TURNER and R. C. SMITH, *Laser in Chemistry Conference,* Royal Institute, London (1977).
9. D. C. HANNA, P. A. KÄRKKÄINEN and R. WYATT, *Opt. Quant. Elect.* 7 (1975) 115–19.
10. M. A. NOVIKOV and A. D. TERTYSHNIK, *Sov. J. Opt. Quant. Elect.* 7 (1975) 115–19.(2)
11. I. R. BEATTIE, J. D. BLACK, T. R. GILSON, D. GREENHALGH, D. C. HANNA and L. C. LAYCOCK, *Lasers in Chemistry Conference,* Royal Institution, London (1977).